

## Holographic Noise in Interferometers

Craig J. Hogan

*University of Chicago and Fermilab*

General arguments based on black hole evaporation, and on particular interpretations of holographic unification, suggest that there may be a new kind of indeterminacy in the relative transverse position of bodies in spacetime, corresponding to the diffraction limit of Planck wavelength radiation. Suitably designed instruments should display a new phenomenon, resembling a randomly varying shear in relative transverse position away from classical geodesics, with a flat power spectral density at low frequencies given approximately by the Planck time, and with no other parameters. An effective theory is presented to connect holographic unification with macroscopic phenomena, such as the statistical properties of noise in signals of interferometers. Macroscopic position operators in Matrix theory are interpreted to obey a Schrödinger wave equation, or equivalently a paraxial wave equation with a Planck frequency carrier, that connects longitudinal and transverse modes. A model based on gaussian-beam solutions of this equation is used to derive formulas in the time and frequency domain for autocorrelation of beamsplitter position in a Michelson interferometer. The equivalent spectrum of gravitational wave noise is estimated for an interferometer with folded arms. The cross-correlation of signals in two non-coincident interferometers as a function of separation is estimated. The cross-correlation signature may be exploited in the design of experiments to provide convincing evidence for or against the holographic hypothesis.

### INTRODUCTION

In quantum mechanics, a particle of energy  $E$  has a frequency  $\nu = \omega/2\pi$  given by Einstein's photoelectric formula  $E = h\nu = \hbar\omega$ , where  $h$  is Planck's constant. By contrast, in General Relativity a given quantity of mass-energy is associated with a minimum length, the Schwarzschild radius  $R_S = 2GE/c^4$  of a black hole, which sets a maximum frequency. These criteria collide at the Planck scale, conventionally defined as  $\lambda_P/c \equiv t_P \equiv \sqrt{\hbar G_N/c^5} = 5.4 \times 10^{-44}$  seconds, setting a minimum time interval or wavelength, or maximum frequency, where physics can be consistently described using quantum particles and fields on a classical spacetime background.

Traditionally the Planck frontier has been identified as a UV cutoff in field theory in 3+1D spacetime. A consistent theory of mass-energy and spacetime cannot be achieved simply by imposing a UV cutoff in 3+1D, filtering at the Planck length in some classical lab frame. A Planck length ruler in some lab frame will, in some other lab frame boosted along its length, appear shorter, violating the minimum-length restriction. The reconciliation must be achieved by a new unified theory that includes new, unfamiliar transformation properties.

The new idea here is to identify the Planck scale as a maximum frequency in any frame, and then to assert that observable positions of mass-energy in 3D space in that frame are defined by waves with that frequency limit. The paths that connect events in classical spacetime have the same status that rays have as an approximate description of a configuration of a system of waves. The rays corresponding to a system of waves however have a fundamental indeterminacy imposed by diffraction limits. Classical paths can be precisely defined from a system of wavefronts using Fermat's principle, equivalent to a least-action principle or path integral approach, but this does not change the physically observable fact that the energy (or intensity, or probability) is not sharply focused into lines and points. A time-averaged classical metric can be sharply defined mathematically, but does not capture these real physical fluctuations. The diffractive blurring in such a system occurs on a scale much larger than the Planck length.

The hypothesis presented here about macroscopic position states may describe the macroscopic limit of holographic unified theories[1, 2, 3]. In holographic theories, the world is encoded on two dimensional null sheets with one degree of freedom per 4 Planck areas, the same as the entropy of the null surface representing a black hole event horizon. Although there are candidates[4] for holographic theories of everything, it is not generally agreed how they map onto a system resembling a nearly-flat, macroscopic, classical spacetime. The formalism presented here may serve as a phenomenological layer of theory to describe this connection and calculate observable consequences.

Suppose there is a maximum spatial frequency at the Planck scale in any frame. That means that the spatial wavefunction of a macroscopic body does not contain physical components at higher spatial wavenumbers. The wavefunction of position in a particular dimension, say  $z$ , can be expressed as a sum of modes with a cutoff at this

scale. If this were an ordinary wavefunction, it would correspond to a limit on the total momentum of any body at the Planck scale, which is not physical. We suppose instead that the frequency-limited wavefunction is a new kind of wavefunction, that of the spacetime itself, or more precisely, that of the position of massive bodies within the spacetime, relative to a classical trajectory. The new effect therefore does not involve a quantization of spacetime, or indeed any perturbation of the metric; instead, it reflects how mass-energy fields are localized and positions are defined using Planckian waves in a given frame.

At macroscopic separation along the measured  $z$  direction, relative positions of bodies are defined by a wavefunction with a Planck frequency cutoff. Measurements of their position with null waves in the  $z$  direction can be made with Planck precision. However, once the  $z$  direction is chosen as the holographic frame, the relative position wavefunctions in the transverse  $x$  and  $y$  directions, at macroscopic  $z$  separation, are much less well defined. At a separation  $L$  in the  $z$  direction, the transverse uncertainty is of order  $\sqrt{\lambda_P L}$ . This “holographic uncertainty” in spacetime is much larger than the Planck length in the transverse directions. The state of the system, which in this case is the state of the spacetime, depends on the measurement, which fixes the orientation of the holographic frame.

An effective theory of this uncertainty presented here, based on the paraxial wave equation, is motivated on general grounds, and also by a particular interpretation of one holographic candidate theory for unification, Matrix theory. The macroscopic position of mass-energy in some chosen frame is described as a wavefunction. Once a lab frame and a holographic wavefront frame are chosen, the wavefunction is represented by a complex phasor relative to a carrier wave at the Planck frequency. The wavefronts of the carrier define a holographic or wavefront frame. The solutions of the equation define wavefunctions of relative positions within this system, and the eigenstates show explicitly the link between transverse and longitudinal position. The effective theory describes eigenstates of relative position in an emergent spacetime with a limiting frequency. The holographic uncertainty is precisely characterized by the transverse correlations in the wave theory, exactly like those described as diffraction in wave optics.

The Planck scale in the energy domain lies far beyond the reach of current experimental techniques. However if the hypothesis put forward here is correct, it may be possible to study Planck scale phenomena in the spacetime domain, using precise measurements of relative position that are coherent over macroscopic distances. Current technology using laser interferometry may be capable of directly detecting this new, Planck-scale physics, by measuring the relative transverse position wavefunctions of optical elements in interferometers with exquisite precision over macroscopic distances. The positions of optical elements normal to their surfaces are currently measured to a precision such that the average null wavefront curves by only about a Planck length across the measured transverse position error, which is the threshold for these effects to become observable.

The potentially observable new phenomenon associated with these ideas is a universal “holographic noise”: random fluctuations in the relative transverse spacetime positions of bodies widely separated in spacetime, compared to their classical motions, caused in holographic theories by the indeterminacy of Planck-scale waves from which classical spacetime emerges.[5, 6] The power spectral density of this noise given just by the Planck time, with no parameters aside from numerical factors that depend on a particular experimental setup. The paraxial-wave theory is used here to make statistical predictions for the effective positions of optical elements and for the time series of signals in Michelson interferometers. Holographic noise has a precisely characterized frequency spectrum and an absolutely calibrated normalization from black hole physics, with no parameters. It also exhibits a new, distinctive spatial shear character, unlike metric perturbations that correspond to strain motions, like gravitational waves. In addition, signals in two nearby interferometers with no physical connection are shown to be highly correlated, a distinctive signature for designing an apparatus to provide convincing evidence for or against the effect.

The effect discussed here is fundamentally different from previously conjectured fluctuations of a quantum-gravitational origin (e.g., [7, 8, 9, 10, 11, 12]). At the most basic level, those analyses are based on various hypotheses about quantum perturbations of a metric. Holographic noise is not due to perturbations of a metric, but to a new kind of in-common movement of mass-energy relative to a classical metric. All the effects discussed here are described as variations of position, using a mass-energy position wavefunction relative to a fixed, flat metric, and emerge only insofar as positions are defined by measurements of mass-energy. For this reason it is also not the same as gravitational radiation, nor is it “quantum gravity”, or metric fluctuations derived from noncommutative geometry; the spatial character of the fluctuations is distinct from all of these. Indeed, over limited timescales, holographic noise violates the equivalence principle; the position of mass-energy, measured in the transverse direction relative to the separation between events, jitters randomly with time relative to nominal classical geodesics. On the other hand, it respects the equivalence principle on average, and with respect to different forms of energy. It also respects Lorentz symmetry along the longitudinal or propagation direction of particles and radiation, so it does not add dispersion observable in arrival times. Since holographic uncertainty addresses not spacetime on its own, but properties of mass-energy positions that are inseparable from those of a spacetime defined by interactions of mass-energy, it is a hypothesis about a possible observable macroscopic consequence of unification.

## HOLOGRAPHIC INDETERMINACY

Classical spacetime is described as a continuous manifold of events. This is an approximation to reality. A real spacetime cannot be observed directly but only by measurements of mass-energy within it. Particles and bodies are assigned classical positions, and fields are described as functions of classical coordinates, but these coordinates should not be regarded as physically real except insofar as they are measured.

In quantum mechanics relative positions are ill defined because of Heisenberg uncertainty. A quantum state is described by a position wavefunction, the amplitude for a body to be measured at each position. This uncertainty is smaller if positions are measured using massive bodies. In the analysis herein, the Heisenberg uncertainty is neglected; in other words, the ordinary wavefunction of bodies is assumed to be narrower than the Planck length.

However, there is an additional indeterminacy attached to relative positions if there is a maximum frequency or minimum fundamental time. In this case, it is unphysical to describe a position wavefunction as a function of a classical position variable. Instead, a wavefunction for a position observable, or more precisely the amplitude for observing a particular relationship of relative position between bodies, must take account of the frequency limit on their wavefunctions in some observation frame. This ambiguity is best described as a wavefunction for the spacetime itself since it occurs for any possible measurement of relative spatial position. In this view, nearly the same spacetime wavefunction applies to any bodies sharing nearly the same spacetime and the same observation frame.

Holographic indeterminacy is a particular hypothesis about how this works phenomenologically. The observation frame includes a choice of direction, and is expressed by writing a spacetime wavefunction relative to a Planck-frequency plane carrier wave representing that frame. We begin with general descriptions of the effect and its motivation, and follow with a more formal effective phenomenological theory.

### Quantum limit of a Planck wavelength interferometer

Classical spacetime is defined by a metric that describes the distance between events. However, neither the spacetime nor the events are directly observable. Measurements require interactions of particles and waves.

The limits of the classical picture are illustrated well by considering a Michelson interferometer using Planck frequency radiation. There is unavoidable indeterminacy in defining a metric by measuring positions in spacetime with this setup. We conjecture that this is actually a fundamental limit. Since there is no operational way to define spacetime event locations better than this limit, the same uncertainty should appear in any apparatus.

Consider just the uncertainty associated with the position of a beamsplitter. Wavefronts of Planck radiation reflect off an optical surface of a massive body. The phase of the reflected radiation depends on the position of the surface in the direction normal to the surface. At a beamsplitter, the reflected radiation changes direction so the phase depends on the position transverse to the initial propagation direction. The measured phase at the interferometer antisymmetric port depends on the position difference of the beamsplitter in the two arm directions, at different times corresponding to the two reflections off the beamsplitter.

Consider first just a single quantum. The wavefunction splits at the beamsplitter (half reflects, half transmits), propagates along both arms and back, and the squared modulus of the summed amplitude is measured at the antisymmetric port.

Two kinds of uncertainty enter into the measured phase signal. The first is the standard Heisenberg uncertainty in measuring the position of the beamsplitter. Each of the two reflections of the particle state off the beamsplitter, which occur at times separated by  $2L/c$ , occur at positions uncertain by  $\Delta x_1 > h/\Delta p$ , where  $\Delta x_1$  denotes the standard deviation of the beamsplitter position and  $\Delta p$  denotes the standard deviation in the momentum of the reflected particle associated with each reflection. (In this analysis we omit numerical and trigonometric factors of order unity to clarify the essential scalings.)

The second part of the uncertainty in the signal is associated with the fact that the different momenta of the waves in the two arms leads to a difference in relative phase when they are recombined and detected. Because of the slight difference in frequencies the number of wave cycles in the two arms do not agree. The uncertainty in apparent arm length difference from this part is then  $\Delta x_2 > 2L\Delta p/p$ .

Several features are notable. The combined uncertainty is a result of the wavelike character of the measurement, and is not there if we time the flights of a classical pointlike particle travelling along rays in a classical background. The group velocity of a relativistic wavepacket does not change speed with a change in momentum, so a timing measurement of a particle eigenstate along one axis relative to a perfect clock would not reveal the uncertainty. On the other hand, if we use wave cycles along each arm to measure the flight time along the other, there is uncertainty.

Also, the transverse character of the position measurement matters: the second uncertainty is not there there if the two arms are aligned along the same axis, because the phase displacements are the same.

Still omitting numerical factors of order unity, the total variance in the arm length is then the sum of the two terms:

$$\Delta x^2 > (h/\Delta p)^2 + (L\Delta p/p)^2. \quad (1)$$

The variance in the sum is minimized when the two terms are equal. This leads to an uncertainty in apparent position difference,

$$\Delta x > \sqrt{Lh/p} = \sqrt{\lambda_P L}, \quad (2)$$

where we set the carrier wavelength to the Planck value,  $\lambda_P = h/p$ .

As discussed below, this  $\Delta x$  is also the waist size for the Planck radiation beam, as determined by diffractive wave optics; the phase of a wavefront with radius of curvature  $L$  changes by unity over patch of transverse size  $\sqrt{\lambda_P L}$ . However, it is not the uncertainty in where the particle reflects off the beamsplitter that matters; in fact, this is not measured. It is the position of the wavefronts, and the position of the beamsplitter itself at the time of the two reflections, that affect the measured phase.

With coherent radiation including many quanta, the standard quantum uncertainty is reduced. With  $N$  quanta in the same state, the first uncertainty becomes  $\Delta x_1 > h/N\Delta p$ , because all the quanta participate in a single measurement. The second remains  $\Delta x_2 > 2L\Delta p/p$  as before because the phases of the coherent quanta are the same. Now the overall uncertainty is

$$\Delta x^2 > (h/N\Delta p)^2 + (L\Delta p/p)^2, \quad (3)$$

which creates a minimum uncertainty

$$\Delta x > \sqrt{Lh/Np} = \sqrt{\lambda_P L/N}. \quad (4)$$

A laboratory interferometer uses this feature to reduce the quantum uncertainty in measurement. However, Planck radiation cannot have an occupation number greater than unity and must be incoherent. In this case the phase of each quantum is independent. For a measurement with  $N$  independent quanta, the first uncertainty becomes  $\Delta x_1 > h/N^{1/2}\Delta p$ , because each quantum makes an independent measurement and the accumulated perturbations add in quadrature. The second becomes  $\Delta x_2 > 2L\Delta p/N^{1/2}p$  because the mean phase displacements add in quadrature. The minimum uncertainty is not reduced in this case, so the Planck interferometer has an irreducible uncertainty in measured phase, corresponding to a standard deviation in beamsplitter position wavefunction (or arm-length difference) given by Eq. 2.

We have discussed this effect as if it is a standard Heisenberg position uncertainty created by Planck waves in a classical background, with an extra limit imposed on phase density of quanta. It describes the best measurement possible of relative positions in spacetime, given the limitations of interactions of mass-energy with a Planck frequency cutoff. The limits on frequencies and spatial wavenumbers are connected with the unification of spacetime and mass energy. One interpretation of the uncertainty is that this is actually a fundamental limit on the definition of positions of mass-energy within a spacetime, and therefore on the definition of a classical metric where positions of events must always be operationally defined by interactions of mass-energy. In this case the phase uncertainty results from a new kind of uncertainty principle due to unification physics. This argument suggests that interferometers may offer a route to Planck scale physics because the uncertainty is magnified in a macroscopic apparatus to much larger than the Planck length.

Currently, optical-wavelength interferometers can reach the Planck quantum limit because they can measure the mean position of a massive body to this precision over a large surface area, macroscopic on a scale of millimeters to centimeters, with very large numbers of coherent quanta, at their standard quantum limit. The hypothesis explored here is that optical interferometers are still subject to the Planck bound because of new physics described by holographic unification. As shown below, the holographic hypothesis also suggests another feature—that the displacements are coherent on scale  $\approx L$ , even with no physical connection.

### Quantum Description of the Effect

Holographic indeterminacy can be derived straightforwardly from the wave mechanics of Planck-wavelength particle states[5]. It corresponds to the diffraction-limited uncertainty in transverse position correlations of particle position states.

Consider measurements of the positions of massive bodies at rest in a flat spacetime with a Euclidean coordinate system in some laboratory frame. The  $x$  position of body 1 is measured at time  $t_1$  relative to some distant reference. This measurement places the position of other bodies into a definite quantum state described by a spacetime wavefunction that depends on their positions but not on their other properties. The effect of the measurement propagates at velocity  $c$  from the measurement event. If a position of body 2 is measured on this light cone, the positions of bodies 1 and 2, separated by a distance  $L_{12}$  in the  $yz$  plane, are conjugate operators, related by

$$[x_1, x_2] = -i\lambda_P L_{12}. \quad (5)$$

The width of the wavefunction and probability distribution describing their relative position increases with separation like  $\Delta x_1 \Delta x_2 = \lambda_P L_{12}$ .

This new form of indeterminacy can be described using wave mechanics of position relative to a Planck wavelength carrier wave in the lab frame[5]. A spatial localization of a body by a measurement creates a momentum uncertainty in the same direction. This creates perturbations in the orientation of carrier wavefronts that propagate to create a transverse uncertainty at large distances. The nonlocal propagation of the effect can be described using diffraction theory, described below.

A measurement collapses the wavefunction to produce a random effective “motion” — not an ordinary motion, but a change of relative position that depends on a choice of frame. The character of the resulting effective motion is that of a shear: matter along any given line moves together, relative to that along other parallel lines, by an amount corresponding to a random walk of about a Planck length per Planck time in the transverse directions, that is, within a null wavefront plane. The calculation of interferometer response below is based on such a semiclassical model.

### Semiclassical Description of the Effect

If the wavefunction of the macroscopic spacetime states is collapsed by the environment on a continuing basis, the effect can be described semiclassically, as a shear motion corresponding to a random walk. Although it describes a real and observable change in position, the movement is not ordinary classical motion, and the randomness is fundamentally quantum in nature.

In a holographic flat spacetime, the world is encoded, at Planck resolution, on a single 2D reference plane that appears, in any lab frame, to be moving at the speed of light. The transverse position of mass in another parallel plane at distance  $L = ct$ , relative to mass in the reference plane, is described by a wavefunction with a standard deviation  $\approx \sqrt{L\lambda_P}$ , the Rayleigh diffraction scale for Planck wavelength waves at distance  $L$ . The choice of a reference plane determines a set of eigenstates, which we call a holographic frame. If a measurement extends over a macroscopic distance  $L$ , the position wavefunction built from these eigenstates displays an inherent indeterminacy in relative transverse positions of order  $\approx \sqrt{L\lambda_P}$ .

By the same token, if the wavefunction collapses on a continuous basis, it implies that in a particular lab frame, there is a random variation of position with time. The relative transverse position of bodies separated by a distance  $L$  varies over time, like a bounded random walk, of a Planck length per Planck time. This spreading saturates however: at times separated by more than  $L/c$ , the relative measured position of the two bodies “at rest” is drawn from a distribution around a fixed classical position, with a width  $\sqrt{L\lambda_P}$ . Nearby bodies, separated by much less than  $L$  in the transverse direction, experience nearly the same apparent motion relative to distant ones.

Consider events in a flat spacetime with a Euclidean coordinate system in some laboratory frame. Observer X sets up two pointlike bodies with separation  $L$  along the  $x$  axis. This is done by timing pulses of reflected radiation from a body at the origin, which we call the beamsplitter, to an end body. Observer Y sends a pulse from the beamsplitter along the  $y$  axis to an end body at the same distance  $L$ . The bodies are massive enough that we can neglect standard Heisenberg quantum uncertainty in their position. Classically, the system can be prepared in this way with everything at rest in the lab frame. With holographic indeterminacy however, if pulses are sent out at the same time along the two axes, they do not return at the same time.

Consider the X frame. Photons always move at exactly  $c$  in the lab frame. At the moment  $t = L/c$  when the pulse reaches the body at  $x = L, y = 0$ , the pulse along the  $y$  axis is at  $y = L, x = 0$  in the laboratory coordinates. However, in this frame the bodies along the  $y$  axis— both the beamsplitter and the end mass— are not at their classical positions, because they are in a plane a distance  $L$  from the reference plane. They are both displaced by about  $\Delta y \approx \sqrt{L\lambda_P}$ . This is described quantum-mechanically, using a wavefunction of transverse position for the center of mass of this plane. At time  $2L/c$  in the classical system, the pulse would return to the beamsplitter:  $x = y = 0, t = 2L/c$ . However, the return  $y$  pulse reaches the beamsplitter at a different time. It reaches  $x = y = 0$

at the time  $t = 2(L + \Delta y)/c$ . The same description applies in the Y holographic frame, with X and Y labels reversed. Each time this measurement is performed,  $\Delta y$  and  $\Delta x$  are both different, drawn from a distribution of standard deviation  $\approx \sqrt{L\lambda_P}$ . Although we have chosen  $x = y = 0$  as a reference point for the beamsplitter position, the effect on arrival times is the same as holding the end bodies fixed in the lab frame and having a random motion of the beamsplitter.

The effective movement is both approximately rigid and transverse, so it does not create differential motions of adjacent bodies in the same transverse direction on the same null sheet, even though it does create differential motions of bodies for events with timelike separation. Indeed it is clear that it is not an ordinary movement at all. Unlike interaction with gravitational waves, no energy is exchanged between the spacetime and the photons doing the measurement.

A Michelson interferometer implements this thought-experiment by interfering light from two orthogonal paths. A wavefront interacts with the beamsplitter twice, first reflecting along one arm and then, a time  $2L/c$  later, from the other. Between these reflections the beamsplitter “moves” as just described. The phase of the interference signal on short timescales behaves as if the beamsplitter, but not the other optical elements, randomly moves by about a Planck length per Planck time. For time intervals longer than  $2L/c$  the apparent random motion is bounded, the width of the distribution given by  $\approx \sqrt{L\lambda_P}$ .

This description is helpful to understand the effect on interferometers of different layouts. For example, in unequal arm interferometers, the noise is determined by the shorter of the two arms. Similarly, interferometers optimized to detect gravitational waves, which often have either folded arms or resonant cavities to amplify strain response, are not necessarily optimized to detect holographic shear noise. Another important feature is that if there is more than one interferometer, nearby optical elements sharing the same null wavefront share the same holographic displacement, even if they have no physical connection. As discussed below, these features are important in designing a system to show this effect and exclude other sources of noise.

### General Arguments for Holographic Uncertainty

The new holographic uncertainty in the relative transverse position of macroscopic bodies is motivated by arguments that are less precise, but more direct, than the wave theory used below to compute the effect.

#### *Direct Derivation from Black Hole Evaporation*

Holographic unification was originally motivated by black hole physics, in particular, Hawking’s discovery that black holes evaporate. This process offers insights into unification because the entropy of the black hole event horizon—an object defined by properties of a pure vacuum solution of classical relativity—is converted into the entropy of ordinary particle quantum states in a flat spacetime background. The holographic principle adopts the view that the entropy of an event horizon exemplifies a general property of all null surfaces. We can use this system to study holographic degrees of freedom of macroscopic position.

In Hawking evaporation, degrees of freedom of a black hole are converted to free particle states. A typical final evaporated state has no black hole; it is a nearly empty vacuum spacetime with about the same number of particles as the number of Planck areas in the original event horizon. Holographic uncertainty can be derived directly from the requirement that black hole evaporation obeys quantum mechanical unitarity. Here we sketch the argument without numerical factors of the order of unity, although it should be possible to calibrate the predicted uncertainty with a more careful calculation. The number of degrees of freedom of the position eigenstates of particles evaporated from a black hole must agree with the degrees of freedom of the hole.

Consider a black hole of radius  $R_S$ , in the center of a giant spherical shell of photographic film of radius  $L$ . After a long time, the hole has evaporated. Each evaporated particle has left an image on the film. In principle the arrival times can be recorded so different arrival times correspond to different states. There are about  $N \approx (R_S/\lambda_P)^2$  particles altogether. At the time a particle evaporates, its wavefunction is close to isotropic (an s-wave state); however, by capturing the images on the film, we have changed basis and converted the system to one where the particles are eigenstates of position, or more precisely, angular direction relative to the hole.

The number of states of the evaporated particles cannot be more than the number of states of the hole. We show that this works out about right if the distant, flat spacetime has a new holographic uncertainty in transverse position independently of the properties of the hole.

We can think of the hole as covered in Planck size pixels. In thermal evaporation, every time  $\approx R_S/c$ , the hole is reduced by the typical thermal particle mass  $\approx \hbar/R_S c$  and shrinks by one Planck area. The number of different ways to disassemble the hole is the number of ways this can happen  $N$  times over. It equals the number of evaporated states if for each particle the number of final directional eigenstates is also  $N$ . (Every time  $R_S/c$  there are  $N$  choices of direction. This happens  $N$  times before the hole is gone so there are  $N^N = \exp N \log N$  states. The entropy is then  $N \log N$ . If the difference in ordering is ignored, the entropy is just  $\approx N$ . The ordering factor cancels in the comparison of the hole with the distant film.) Every evaporation time  $R_S/c$  there are  $N$  choices of direction, and this has to match the number of options for the image location for that particle in the final image.

Suppose there is an uncertainty  $\Delta x$  in the transverse positions of the particle images, so that the information, or number of degrees of freedom in the film image is  $(L/\Delta x)^2$ . The film can have much finer grain pixelation in local measurements; local physics is not changed. The new uncertainty refers to a new relative uncertainty in transverse position over large distances  $\approx L$ , requiring a nonlocal measurement in space or time. In the case of evaporation, it is a new uncertainty in positions of images relative to the center of the hole. Nearby images, formed at nearly the same time, share the same “holographic displacement”. Images far apart in time or space have added indeterminacy or noise in relative position because the hole states cannot specify what they are.

The number of evaporated particle states matches the number of black hole states if  $(L/\Delta x)^2 \approx (R_S/\lambda_P)^2$ . There is no contradiction with the black hole entropy as long as

$$\Delta x^2 > L^2 \lambda_P^2 / R_S^2. \quad (6)$$

If  $\Delta x^2$  were smaller than this, then the amount of information per evaporated particle would be larger than that available in the hole. It would take more data to specify the final state than is available in the initial state.

Now in addition, the ordinary Heisenberg uncertainty tells us that for the particles of energy  $\hbar c/R_S$ , typical for the evaporated particles, there is already a minimum transverse uncertainty in the image location,  $\Delta x > R_S$ , that is, the images are not sharper than a particle de Broglie wavelength. Then we get

$$\Delta x^2 > L \lambda_P, \quad (7)$$

which is just the holographic uncertainty at distance  $L$ . This uncertainty does not depend on  $R_S$  or any property of the hole, only on  $L$ , so we identify it once again as a property of flat spacetime. Formally we may take  $R_S$  to vanish and require that black holes of any size have unitary evaporation.

Again, the uncertainty is not observable locally— there is no new “fuzziness” in a small patch of the distant film. Rather, the relative angular positions of widely separated images formed are fuzzy, in a coherent way relative to each other, or relative to the position of the hole. If images form within a time  $\ll L/c$  of each other and are physically near each other, they share the same holographic displacement; thus the uncertainty is not observable in any measurement on a scale  $\ll L$ .

If positions in flat spacetime have this transverse indeterminacy, in addition to the Heisenberg uncertainty, then a black hole of any size can leave behind a state with the same size Hilbert space it started with. Since the uncertainty in the distant space does not depend on any property of the hole, it must apply to positions in the spacetime even if there is no hole at all.

### *Holographic Uncertainty from Counting Position Eigenstates*

Holographic noise can be regarded as a sampling noise due to the Planck frequency limit of spacetime, or as the consequence of measuring conjugate observables in a system described by specific, finite number of degrees of freedom. In holographic theories, a bound on the number of degrees of freedom leads to a limit on the number of independent measurable transverse relative positions of macroscopic bodies in an extended system. The signal of an interferometer that compares two transverse positions displays noise as a direct consequence of the frequency bound of the fundamental theory. Conversely, a lack of quantum noise in position observables at a certain level would imply a lower bound on the number of degrees of freedom.

Consider a fundamental theory with these features:

1. *Frequency bound.* In any laboratory frame, there is a maximum frequency  $c/\lambda \equiv \omega/2\pi$ .
2. *Holographic information bound.* On any light sheet, there is a minimum wavelength  $\lambda$  in the transverse directions.

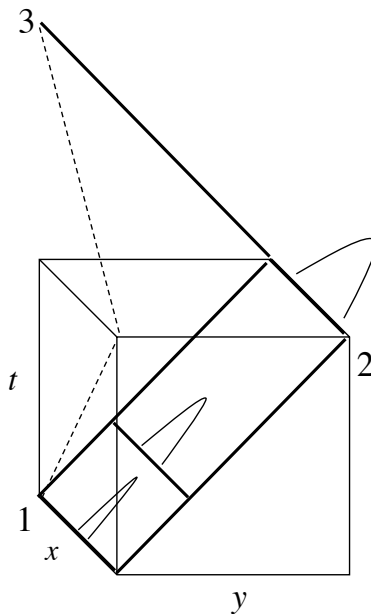


FIG. 1: Holographic spacetime, with  $z$  dimension suppressed. An  $x$  segment of a null sheet normal to  $y$  is shown, generating the emergent  $y$  dimension. The growth of transverse uncertainty is shown schematically. The dashed line shows another null trajectory, normal to  $x$ , as in the orthogonal arm of a Michelson interferometer.

These features are related properties in holographic theories built on light sheets. In a lab frame, we can think of  $c/\lambda$  as the frequency of a carrier wave. In a holographic theory, this does not result in a simultaneous resolution of  $\lambda$  in all three dimensions everywhere at once; rather, this resolution is achieved within a 2D light sheet, which determines the holographic frame, only at single longitudinal position, and in the normal direction to it. When  $\lambda$  is identified with the Planck scale, such a theory approximately satisfies by construction holographic entropy bounds derived from black hole physics. Put another way, these features would be expected in any theory where the thermodynamical properties (such as entropy) of a black hole event horizon arises out of statistical mechanics, from quantum-mechanical degrees of freedom of spacetime.

Consider the situation illustrated in the spacetime diagram, Figure (1). This shows two dimensions of space and one of time in a lab frame; the  $z$  spatial dimension is suppressed. The inclined plane shows a segment of the  $x$  axis moving along a null trajectory, corresponding to the light sheet frame with wavefronts normal to  $y$ . In this frame, all events in this sheet occur at one time; that is, properties of the system at all  $x, y$  on this sheet are encoded holographically by the theory by data along the segment of  $x$  at  $y = 0, t = 0$ . Quantum relationships in this system between events at large  $y$  separation are encoded in this holographic frame by transverse correlations along  $x$ .

A simple way to derive the uncertainty is to count position degrees of freedom. In the standard classical interpretation of quantum mechanics, the number of position configurations cannot exceed the number of states of the system, which means that the number of different position eigenstates for a particular body cannot exceed the number of degrees of freedom of the system. A position state can be expressed as a linear combination of a finite number of such eigenstates.

The Shannon sampling theorem tells us that two numbers per  $\lambda$  suffice to describe any function with no frequencies above  $c/\lambda$ ; thus, along the transverse dimension  $x$  there is a maximum of two position eigenstates per  $\lambda$ . Consider positions in the  $x, y$  plane, without regard to their  $z$  position. The number of position eigenstates in the 2D  $x, y$  plane cannot exceed the information bound in the one  $x$  dimension that sweeps it out:  $N < 2L_x/\lambda$ , where  $L_x$  is the length of the  $x$  segment. But that number of eigenstates now has to suffice to describe positions in a two-dimensional system, the null  $x, y$  sheet.

Now suppose that an apparatus of size  $L = L_y = L_x$  measures the relative positions of bodies in the  $x, y$  plane in the lab frame. For example, a Michelson interferometer with  $x$  and  $y$  arms as shown in figure (1) compares transverse wavefunctions in two different null frames, by combining light at event 3 from the two arms. Suppose that the number of position eigenstates in the  $x, y$  plane corresponds to mean separation  $\Delta x$  in each direction. The number of position eigenstates is  $L^2/\Delta x^2 = N = 2L/\lambda$ , so  $\Delta x^2 = \lambda L/2$ . A time series of such measurements wanders over time  $L/c$  by an amount  $\approx \Delta x$ , yielding a power spectral density for position,  $\Phi \approx \Delta x^2 L/c \approx L^2 \lambda/2c$ ; the dimensionless shear



$\Delta L/L$  has a power spectral density given by the fundamental time,  $\approx \lambda/c$ . This result approximately reproduces holographic uncertainty and noise derived in other ways.

The number of position eigenstates of an interferometer with holographic indeterminacy and noise approximately saturates the holographic bound on degrees of freedom, as derived from black hole physics, if  $\lambda \approx ct_P$ . If holographic noise is not present in a Michelson interferometer, it implies that the system has more eigenstates for positions of its optical elements than those bounds allow, and rules out this interpretation of holography.

### *Degrees of Freedom of a Massless Field*

In a certain sense, holographic indeterminacy is a general property of any frequency-bounded wave field.

Consider a cubic volume of space with a massless scalar field obeying the linear wave equation with reflecting walls. It is conventional to decompose solutions into discrete sinusoidal modes that fit in the box. Given an upper bound on wave frequency, the number of modes is proportional to the 3D volume.

When such a field is quantized, the modes are identified as harmonic oscillators and separately quantized. Each one is identified as a degree of freedom. Thus, the number of degrees of freedom appears to be proportional to volume. Each mode has a number operator and this is one way to decompose the quantum states of the field.

This view is however misleading. Field configurations can also be built from a sum of radiation entering along each face of the cube, with a cutoff in transverse wavenumber corresponding to the maximum frequency. The number of degrees of freedom for propagating waves and particles thus appears to be proportional to surface area, not volume.

The reconciliation of these two descriptions is that the 3D modes are not really independent degrees of freedom. The linear decomposition makes it look that way, and certainly one can build any classical solution by adding linear plane wave mode solutions. But the 3D plane waves are not independent quantum degrees of freedom. A given classical field configuration can be described by many different linear combinations. In the quantum particle description of the states, the localization of a particle in the plane of a wave mode to a small patch on one face of the box implies a transverse momentum uncertainty, and therefore an uncertainty in the wavevector direction, so that the mode is not independent of the others with nearly the same orientation.

This picture describes in general terms the holographic transverse position uncertainty, and nonlocality in the degrees of freedom. A more rigorous derivation showing holographic scaling of total entropy in quantum field theory is given in ref.[13].

## **WAVE PICTURE OF HOLOGRAPHIC SPACETIME**

A physically plausible and informative interpretation of holographic theories uses a wave model of emergent spacetime. The relationship between transverse positions at two times can be described by a quantum wavefunction. In quantum wave language[5], the transverse positions at different times along a null path are conjugate observables, like normal position and momentum in ordinary quantum mechanics, with a commutator  $[x_1, x_2] = -ict_{12}\lambda_P$ . Their Heisenberg-like uncertainty relation gives the same result for the wavefunction width as a wave optics calculation. The wavefunction can be computed in the same way as transverse mutual complex correlation of field amplitudes for radiation of frequency  $c/\lambda_P$  in standard wave diffraction theory[6]. The width of the mutual complex correlation, the joint wavefunction of transverse position at points separated by  $ct$ , increases like  $\Delta x \simeq \sqrt{ct\lambda_P}$ .

The wave hypothesis developed here is based on the paraxial wave equation, another well studied tool in optics theory. This more general formulation allows a more direct connection with a macroscopic limit of fundamental theories, such as Matrix theory. Once again, the complex phasor amplitude of that theory is taken as a wavefunction for spacetime position. This allows us to write down specific eigenstate wavefunctions, and spatial solutions with specific forms, such as gaussian beams, to compute experimental predictions.

### **Holographic Hypothesis: Paraxial Wave Equation**

A specific way to formulate the holographic hypothesis is to posit that effective spacetime wavefunctions describing macroscopic position states are solutions not of the 3D wave equation, but of the paraxial wave equation.

In the emergent 3D space, the 2D light sheet appears as a wavefront moving at the speed of light. The state is thus naturally described as deviations from the wavefronts of a periodic plane wave. The frequency of the carrier is the fundamental frequency in some given lab frame.

Start with the standard 3D wave equation for a field with a single fixed frequency. In three dimensions, the 3D wave equation for any field component can be written as the modulation of a carrier wave,

$$(\nabla^2 + k^2)E(\vec{x}) = 0. \quad (8)$$

Here  $E(\vec{x})$  is a complex phasor representing the amplitude and phase at each point. We use Euclidean coordinates  $\vec{x} = x, y, z$  to denote positions in an arbitrary lab rest frame. A sinusoidal time dependence is built in,  $E \propto \sin(\omega t)$ , where  $\omega = ck = 2\pi c/\lambda$ . In holographic geometry the carrier is at the Planck frequency.

To derive the paraxial wave equation, we express the field in the form

$$E(x, z) = u(x, z)e^{-ikz}. \quad (9)$$

The field  $u$  now describes deviations from a plane wave normal to the  $z$  axis. For simplicity, we consider one transverse dimension  $x$  and one longitudinal dimension  $z$ ; identical and independent equations apply to  $y, z$ . In laboratory optics applications,  $z$  corresponds the direction of a beam, and  $x$  to the width of a beam. In our holographic application  $z$  corresponds to position in a particular direction that defines the normal axis of a holographic frame, and  $x$  to position in a transverse dimension. The wave equation for  $u$  becomes

$$\partial^2 u / \partial x^2 + \partial^2 u / \partial z^2 - 2ik \partial u / \partial z = 0. \quad (10)$$

The paraxial approximation is to assume that the second term is negligible compared with the others:

$$\frac{\partial^2 u}{\partial x^2} - 2ik \frac{\partial u}{\partial z} = 0. \quad (11)$$

This equation is proposed as an effective wave equation governing transverse position states of mass-energy relative to classical spacetime on macroscopic scales.

It should be emphasized that this phenomenological description is not a fundamental theory. The carrier field is not a dynamical physical field, but a calculational tool. It is constructed to represent the holographic behavior in a lab frame; thus, the wavefunction represents the slowly varying parts of the spatial behavior relative to a Planck frequency plane wave. A true carrier field would not be invariant under boosts to another frame, and neither is this; the wavefunctions are frame-dependent. Similarly, the expansion in paraxial coordinates makes sense if the fundamental theory is built on 2D light sheets, even if the actual wavefronts are not the same in a different lab frame. The theory accurately describes the kind of macroscopic geometrical information that is likely to survive in the classical limit, and therefore is motivated as a proposal for an effective theory.

#### *Relation to Matrix theory*

It will be noticed that Eq. (11) is mathematically identical to the one dimensional nonrelativistic Schrödinger wave equation, with  $z$  replacing time and  $-k$  replacing  $m/\hbar$ . The interpretation of this equation as a wave equation for spacetime also appears to be a natural consequence in a particular macroscopic interpretation of Matrix theory proposed in ref.[14]. In this interpretation the single transverse coordinate operator  $\hat{x}$  refers to the center of mass of a collection of  $N$  D0 branes or particles, described as the trace of a fundamental  $N \times N$  matrix, one of nine matrices out of which emerge nine spatial dimensions:  $\hat{x} = \text{tr} \hat{X}$ . The emergent 3D system has a maximum frequency equal to the inverse periodicity  $R$  of the compactified  $M$  dimension, the only scale in the system, assumed in this interpretation to be of order the Planck scale in any lab frame of the emergent spacetime. Modes in the 9 spatial dimensions that emerge from the matrices are not independent on scale  $R$ , where the theory is strongly coupled, which indicates that it obeys the holographic bound[4, 14]

The kinematic terms of the Banks et al.[4] Matrix Hamiltonian for the  $\hat{X}$  matrix can be written

$$\hat{H} = \frac{R}{2\hbar} \text{tr} \hat{\Pi}^2, \quad (12)$$

where  $\hat{\Pi}$  denotes the conjugate to  $\hat{X}$ . This leads to a Schrödinger wave equation resembling Eq. (11) if we make operator identifications similar to those in the standard Schrödinger wave theory, with substitution of the light sheet coordinate  $z^+ \equiv (z + ct)/2$  for  $t$  in the Hamiltonian operator (since for events on a null trajectory,  $z^+ = ct = z$ ):

$$\text{tr} \hat{\Pi}^2 \rightarrow -\hbar^2 \partial^2 / \partial x^2, \quad (13)$$

$$\hat{H} \rightarrow i\hbar\partial/\partial z^+, \quad (14)$$

and set  $R \rightarrow k^{-1} = \lambda/2\pi$ . As in ref. [14], we leave the minus sign in the squared momentum operator, or equivalently, adopt the usual Schrödinger imaginary momentum,  $-i\hbar\partial/\partial x$ . The wave equation for M theory in one transverse dimension then becomes:

$$\frac{\partial^2 u}{\partial x^2} + \frac{4\pi i}{\lambda} \frac{\partial u}{\partial z^+} = 0. \quad (15)$$

This effective macroscopic behavior is far removed from the fundamental theory. Nevertheless it offers a useful intermediate layer of interpretive theory that is useful for phenomenology. Like the Bohr model of the hydrogen atom, it may even be wrong, but it leads to a set of tools for precise calculation and may capture essential elements of how new unification physics can leak into macroscopic experiments.

Solutions to Eq. (15) can be expressed as a sum of modes that combine longitudinal and transverse waves:

$$u(x, z^+) = \sum_{k^\perp} A_{k^\perp} \exp -i[k^+ z^+ \pm k^\perp x]. \quad (16)$$

where the wavenumbers of the modes in the two dimensions are related by

$$k^\perp = \sqrt{4\pi k^+/\lambda}. \quad (17)$$

For each mode there is a longitudinal and a transverse wave. For a wavepacket or superposition, describing the position of bodies (the wavefunction for the center of mass of a collection of branes), there is an uncertainty principle in each transverse direction. The conjugate variables in this case are  $x$  and  $k^\perp$ . Their variances  $\langle \Delta x^2 \rangle$  and  $\langle \Delta k^{\perp 2} \rangle$  in a wavepacket obey uncertainty relations of the usual form,

$$\langle \Delta x^2 \rangle \langle \Delta k^{\perp 2} \rangle \geq 16\pi^2, \quad (18)$$

where the inequality is saturated in the case of gaussian distributions. Using Eq. (17) to convert to the longitudinal wave scale, positions with longitudinal separation on scale  $\Delta L^+ \equiv (4\pi/\lambda)(2\pi/\langle \Delta k^{\perp 2} \rangle)$  have a transverse variance

$$\langle \Delta x^2 \rangle > \lambda \Delta L^+ / 2. \quad (19)$$

Note that  $\hbar$  has not been assumed to be unity here: it has cancelled out, leaving  $\lambda$  as the only scale in the theory.

This is interpreted as a new kind of uncertainty. A system with a macroscopic longitudinal extent has an intrinsic transverse indeterminacy of relative position. Since it is formulated here in terms of waves in both directions, it does not directly give the precise uncertainty for an apparatus of with a specified spatial configuration; some other approaches to computing that are suggested below. Still, this line of reasoning connects an effective macroscopic holographic uncertainty to fundamental holographic light sheet theories.

Normally we think of degrees of freedom as almost all residing in independent modes at the microscopic scale. Interferometers are of course exquisitely designed to ignore these and instead measure the envelope wavefunction, the mean or center of mass position of a vast number of particles, on a macroscopic scale. They exclude from the measured signal as many as possible of the internal degrees of freedom that could potentially add more noise. The Matrix-theory view of this is that the signal directly monitors the trace of one of the (very large dimensional) fundamental matrices corresponding to the center of mass of a whole body, and indeed of other bodies with no other physical connection. Thus it is possible for new types of correlations to arise in the wavefunctions and time behavior of separate systems, as discussed below. The holographic character of the matrix Hamiltonian provides a consistent framework that tracks how degrees of freedom change character in different frames; the Planck length ruler never contracts to less than a Planck length in a boosted frame.

### Paraxial Representation of Holographic Spacetime

Wave optics language translates straightforwardly into a hypothesis about the quantum states of an emergent, holographic spacetime. The holographic geometry hypothesis is that macroscopic wavefunctions of position transverse to a light sheet obey the paraxial wave equation (Eq. 11), with a fundamental wavelength  $\lambda$ , in terms of the normal coordinate  $z$  in any lab frame:

$$\frac{\partial^2 u}{\partial x^2} - \frac{4\pi i}{\lambda} \frac{\partial u}{\partial z} = 0. \quad (20)$$

The  $z$  coordinate represents a position along a null trajectory, the emergent direction in the 3D space. In standard Minkowski space coordinates, it is the same as  $t$ ; however, the wave equation is direction-specific.

The interpretation of this equation is that it governs the wavefunction for  $x$ , the center of mass position of a system of particles in one transverse dimension of a flat spacetime. In a particular laboratory frame,  $x$  and  $z$  are standard Euclidean coordinates. The equation refers to a particular holographic frame with wavefronts normal to  $z$ . In this holographic frame, another, independent equation also applies with  $y$  replacing  $x$ .

This is not an equation of motion of the particles in the standard sense: it refers to the quantum wavefunction of position as limited by the holographic nature of unification. The holographic quantum behavior described by Eq.(20) depends not at all on any properties of the particles, except for their relative position: all the usual physics of the field motion and interaction is in addition to this. In the matrix theory argument leading to the paraxial equation, we discarded all the terms describing fermionic activity and noncommutative matrix geometries, and included only the kinematic geometrical terms. The  $x$  coordinate is thus interpreted as the center of mass position of all mass and energy at a longitudinal position corresponding to a wavefront.

### *Gaussian Beam Solutions as Spacetime Wavefunctions*

A set of useful solutions of the paraxial wave equation from wave optics is can be applied to describe transverse position states on wavefronts at null separations. They describe beams that fall off transversely with a gaussian profile. These gaussian beams comprise a one-parameter family of solutions, characterized by a longitudinal distance  $z_R$  (called the “Rayleigh Range”) that physically corresponds to a radius of wavefront curvature at the place where the beam has broadened by a factor of two from its narrowest point. Since the gaussian beams represent the “minimal” transverse uncertainty. For a given set of boundary conditions, they saturate the uncertainty principle, in the sense of having the smallest transverse variance. We adopt these modes as a working model for estimating the level of irreducible, universal holographic noise in interferometers.

In a given holographic frame, the Gaussian solution to (20) can be expressed as[15, 16]

$$u(x, z) = \frac{w_0}{w(z)} \exp \left[ -iz(2\pi/\lambda) - i\phi - x^2 \left( \frac{1}{w^2} + \frac{i\pi}{\lambda R} \right) \right] \quad (21)$$

where

$$\phi = \arctan(\lambda z / \pi w_0^2). \quad (22)$$

In optics the quantity  $R$  represents the real radius of curvature of the wavefronts. The real part of the wavefunction displays a Gaussian profile in the transverse direction  $x$ . The Gaussian width of the beam varies as

$$w(z) = w_0 \sqrt{1 + (z/z_R)^2} = w_0 \sqrt{1 + \left( \frac{\lambda z}{\pi w_0^2} \right)^2}, \quad (23)$$

and the radius of curvature

$$R(z) = z \left[ 1 + \left( \frac{\pi w_0^2}{\lambda z} \right)^2 \right] \quad (24)$$

The width at the  $z = 0$  “waist” for a given solution, corresponding to a flat wavefront, is

$$w_0 = \sqrt{\lambda z_R / \pi}. \quad (25)$$

The width of the beam gradually broadens with propagation due to diffraction. Modes with narrower waists diffract more and broaden more quickly. The minimum transverse width at a distance  $z$  occurs for the mode with  $z = z_R$ . Conversely at a distance  $z_R$ , there is a minimum transverse width,  $\sqrt{2}w_0 = \sqrt{2\lambda z_R / \pi}$ .

A system of spacetime+mass-energy can be put in different states, represented by solutions characterized by  $w_0$  or  $z_R$ , by a measurement apparatus. A small transverse width at the waist implies a larger transverse width at large  $z$ . For a given  $z$  separation between two measurements, there is an optimum state which minimizes the uncertainty in the sum or difference of  $x$  for the two measurements. The Gaussian solution is the least uncertain.

In a theory where states are encoded on light sheets with a characteristic or maximum frequency, the transverse width of the position wavefunction displays this minimum diffractive uncertainty. The  $x$  observable described by this wavefunction is the position of “everything”— the center of mass of all mass-energy on the wavefront.

The gaussian-beam picture invites another characterization of holographic uncertainty: at each separation, it is the minimum width of a coherent beam of Planck wavelength radiation. As noted above, since the occupation number of Planck wavelength states cannot exceed unity, holographic noise corresponds to the standard quantum limit, at the free spectral range, of an interferometer that uses Planck-wavelength radiation.

It is also illuminating to consider the curvature of wavefronts. A wavefront with radius  $R$  bends longitudinally by  $\lambda$  over a transverse width  $\sqrt{\lambda R}$ . Consider a perfectly shaped and measured laser beam wavefront, but assign it a minimum longitudinal width  $\lambda_P$ , that is, a minimum length or maximum frequency in the lab frame. The wavefront position cannot be defined more precisely than this in any experiment. Then the same phase will be measured everywhere in a patch of size  $\approx \sqrt{\lambda_P R}$ . In the wavefunction interpretation, this is equivalent to saying that the position wavefunction is spread over a patch of this size. If the beam interferes with a similar orthogonal beam at a beamsplitter having this wavefunction, the phase difference cannot be measured with higher precision than this width. (Even though the beamsplitter is at the waist of a beam, so the real radius of curvature diverges, the complex part of the position wavefunction still “knows about” the mode radius and imprints a transverse profile on the outcome of a measurement.) In an optical cavity of any arm length, the holographic transverse uncertainty is smaller than the optical beam waist by a factor  $\approx \sqrt{\lambda_P/\lambda_{opt}}$ .

It is also useful to reflect again on the black hole thought experiment. At a distance  $< R_S^2/\lambda_P$  from the hole, the transverse uncertainty of evaporated particles is dominated by the Heisenberg uncertainty, and the gravitational curvature of wavefronts is bigger, that is, with smaller radius than the holographic curvature radius. At larger distance, the holographic uncertainty dominates and is independent of the (at this distance very small) gravitational effect of the hole.

## STATISTICS OF HOLOGRAPHIC NOISE IN SIGNALS

Holographic uncertainty (in analogy to Heisenberg uncertainty) can be defined as the minimum of the product of the widths of transverse wavefunctions  $u$  at some separation  $L$ . The value of the difference of the positions is indeterminate, leading to holographic indeterminacy in an instrument, such as an interferometer, that measures such a difference. Holographic noise comes about because the indeterminacy leads to a random variation in the measured position as a function of time.

### Setting $\lambda$ from Black Hole Physics

The wave theory is normalized by matching degrees of freedom to gravitational physics. We require the theory to agree with the entropy per transverse lightsheet area from black hole thermodynamics,

$$S_H/A = (4\lambda_P^2)^{-1}, \quad (26)$$

where Boltzmann’s  $k$  is set equal to unity.

This entropy corresponds to one degree of freedom per  $2\lambda_P$  in each transverse direction. Standard quantization for a confined scalar particle gives one degree of freedom per  $\lambda$  for each direction. These agree if the effective fundamental wavelength, for macroscopic purposes, is twice the standard definition of the Planck length:

$$\lambda_0 \equiv 2\pi/k_0 \equiv ct_0 = 2\lambda_P \equiv 2ct_P. \quad (27)$$

Henceforth we will normalize to this value for predictions of observable effects.

This may be an exactly correct value for all practical purposes, since it invokes new physics only via gravitational entropy, which is well calibrated with ordinary entropy using the theory of black hole evaporation. However, this derivation falls short of a rigorous proof, and does not offer a detailed characterization of the actual degrees of freedom. A better understanding of the fundamental degrees of freedom, and how they relate to gravity, is one goal of an experimental program.

### Autocorrelation of Displacement

Suppose we have a way of measuring transverse position as a function of time along a light sheet trajectory. In an appropriate setting we can interpret  $u(x, z)$  as a quantum wavefunction and use it to compute the time correlation of the measurements.

We wish to compute the statistical properties of a signal, a scalar phase as a function of time. Suppose that the effect of holographic noise mimics a classical motion of the beamsplitter as described above. Denote by  $X(t)$  the difference in position of the beamsplitter along the two arm directions at time  $t$  in a lab frame. The time correlation of the classical scalar  $X$  is defined as the limiting average,

$$\Xi(\tau) = \lim_{T \rightarrow \infty} (2T)^{-1} \int_{-T}^T dt X(t) X(t + \tau) \quad (28)$$

In a particular interferometer optical configuration (depending on signal recycling, folded arms, Fabry-Perot arm cavities, etc.),  $\Xi(\tau)$  determines the statistics of the noise in the signal.

The two measurement events are on wavefronts separated by  $c\tau$ . We model the wavefunction as a gaussian beam mode where the radius  $z_R = c\tau/2$ . The correlation (Eq. 28) at lag  $\tau = 0$  is given by the mean square displacement determined by the wavefunction (Eq. 21) with  $z_R = c\tau/2$ , with an extra factor of 2 because we add the variance from two events:

$$\Xi(\tau = 0) = 2 \int dx x^2 u^*(x, z = z_R = c\tau/2) u(x, z = z_R = c\tau/2). \quad (29)$$

The standard deviation of each gaussian  $u$  is  $\sigma = w/\sqrt{2}$ ; for their product,  $\sigma = w/2$ . Twice the mean square then is given by  $2w^2(z = z_R)/4 = w_0^2 = z_R \lambda / \pi = c\tau \lambda / 2\pi$ .

In the classical limit, the transverse motion mimics a random walk. For each Planck length of longitudinal propagation, there is a transverse step of about a Planck length, in a random direction, along each transverse direction. In an interferometer of finite size  $L$ , there is a limit to the random walk, corresponding to a cutoff in longitudinal (and therefore transverse) wavenumbers. Let  $L$  denote the length of the arms, so that  $2L$  is the round trip travel time. As illustrated by the wave eigenstates above, over longer times, the signal does not show the holographic noise, since the whole apparatus “moves” together. The random walk for the position observable therefore has a bound imposed at time  $2L/c$ . The time autocorrelation of classical position is then

$$\Xi(\tau) = (ct_0/2\pi)[2L - c\tau], \quad 0 < \tau < 2L/c. \quad (30)$$

The standard deviation saturates at the value for  $\tau = 2L/c$ , so

$$\Xi(\tau) = 0, \quad \tau > 2L/c. \quad (31)$$

These formulas do not capture the correct behavior at very small  $c\tau$ , less than the beam diameter, say. However, for practical purposes Eqs. (30) and (31) are a description of the classical behavior. Time-domain sampling of the signal is predicted to show this correlation.

The behavior can also be described in the frequency domain. The spectrum  $\Phi(f)$  is given by the Wiener theorem,

$$\Phi(f) = 2 \int_0^\infty d\tau \Xi(\tau) \cos(\tau\omega), \quad (32)$$

where  $\omega = 2\pi f$ . [17] Integration of this formula using Eqs.(30) and (31) gives a prediction for the spectrum of the holographic displacement noise,

$$\Phi(f) = \frac{c^2 t_0}{\pi L (2\pi f)^2} [1 - \cos(f/f_c)], \quad f_c \equiv c/4\pi L. \quad (33)$$

The low frequency limit ( $f \ll c/2L$ ) gives a flat spectrum independent of  $f$ :

$$\Phi(f) \approx 2t_0 L^2 / \pi = 4t_P L^2 / \pi, \quad f \ll c/2L. \quad (34)$$

The spectrum at frequencies above  $f_c$  oscillates with a decreasing envelope. The apparatus size—the distance over which the sampling occurs—acts as a high-pass filter; fluctuations from longer longitudinal modes do not enter into the signal.

*Apparent Gravitational Wave Spectrum*

A model of an apparatus using the beamsplitter position correlation function (Eqs. 30, 31) as a description of effective classical motion allows an exact prediction of the signal statistics at all frequencies. Current results are generally quoted in terms of equivalent gravitational wave strain, which requires a consideration of the gravitational wave transfer function of an apparatus.

A gravitational wave is a perturbation of the spacetime metric. As emphasized earlier, the holographic effect is not a metric perturbation, but a fluctuation of mass-energy position from a classical geodesic. A gravitational wave affects interferometer signals by causing a perturbation in the difference of integrated distance traversed by light in the two arms. Holographic noise affects the signals by a physical change of position, a bounded, temporary violation of the equivalence principle. The apparent gravitational wave spectrum of holographic noise depends on the configuration of the apparatus. In particular, it changes if the arms of the interferometer are folded, or include resonant Fabry-Perot cavities that amplify the effect on phase of an arm length perturbation.

In the low frequency limit (Eq. 34), the effective holographic beamsplitter displacement noise in a folded Michelson interferometer creates the same noise spectrum as an amplitude spectral density of gravitational waves,

$$h(f) = \mathcal{N}^{-1} \sqrt{\Phi/L^2} = \mathcal{N}^{-1} 2\sqrt{t_P/\pi} = \mathcal{N}^{-1} 2.6 \times 10^{-22} / \sqrt{\text{Hz}}, \quad (35)$$

where  $\mathcal{N}$  is the average number of photon round trips in the interferometer arms.

The reason for the added factor of  $\mathcal{N}^{-1}$  in Eq.(35) is that folded arms (as in GEO600) amplify the signal response to a gravitational wave strain, but do not increase the holographic noise in the signal. The holographic displacement of the beamsplitter and inboard folding mirrors in physical length units just depend on the actual size of the arms. The folding effectively lengthens the arms for gravitational wave detection by up to a factor of  $\mathcal{N}$ , but it does not change the displacement spectrum or amplify the holographic noise in the signal. Thus for a given physical displacement of the beamsplitter, the measured phase displacement corresponds to a gravitational-wave strain proportional to  $\mathcal{N}^{-1}$  at frequencies below  $\approx c/2L\mathcal{N}$ .

One might worry that the inboard mirrors share the holographic motion of the beamsplitter in their normal direction. This is however already taken into account in the above argument. The holographic movements of the inboard mirrors (if they are close to the beamsplitter) are almost the same as those of the beamsplitter. They execute the same bounded random walk about a common classical position. In equivalent gravitational wave units, the holographic noise appears to be reduced at low frequencies in a folded geometry because a given displacement in the position of inboard optics corresponds to a smaller strain perturbation.

In GEO600, with  $\mathcal{N} = 2$ , the estimate in Eq.(35) predicts a new noise source,  $h = \sqrt{t_P/\pi} = 1.3 \times 10^{-22} / \sqrt{\text{Hz}}$ , at all measured frequencies. This holographic noise spectrum approximately agrees with currently unexplained “mystery noise” in GEO600, above about 500Hz.

In ref. [6] a similar result was derived, by a calculation based on a wave-optics model similar to that presented here. In that paper however it was erroneously claimed that in a power recycling cavity the predicted slope changes at very low frequencies, below an inverse power-recycling time. In fact the apparent gravitational wave spectrum corresponding to a bounded random walk of the beamsplitter is just flat at low frequencies, as in Eq. (35). In addition, the numerical factor in ref. [6] was different,  $h = \sqrt{t_P/2}$  instead of  $h = \sqrt{t_P/\pi}$ , so the predicted noise is now less, by about 20%. The current calculation takes into account the detailed profile of the gaussian mode solution, Eq. (25), which is likely to be a more physically realistic model of instrument/spacetime wavefunction, and should be taken as a more reliable calculation than the earlier one of the actual minimum level of noise. (This exact prediction, however, should still not be considered definitive, since the description of the apparatus is still based on a semiclassical wave model.) With this estimate, low frequency excess noise in GEO600 is still unexplained, but the holographic prediction still approximately fits the unexplained noise above about 500 Hz. Indeed if it is real, holographic noise is currently the dominant noise source in GEO600 at its most sensitive frequency— about half of the measured noise power.

GEO600 is more sensitive than LIGO to beamsplitter displacement, even if it is less sensitive to gravitational waves. The holographic noise predicted in LIGO is below current limits by a significant factor due to its Fabry-Perot arm cavities, which have a finesse corresponding to  $\mathcal{N} \approx 10^2$  round trips. Without the factor of  $\mathcal{N}$ — that is, if noise lacks the specific transverse shear character of holographic noise— current LIGO limits rule out excess noise with this amplitude. For this reason, LIGO data already rule out models predicting Planck-amplitude noise in the metric, which has a strain character[8, 9, 11]. Calculation of LIGO response to holographic noise may however be more subtle than that of GEO600 since the inboard mirrors of the arm cavities are quite close to the beamsplitter so the light freely propagates across a much shorter distance.

The equivalent strain formula (Eq. 35) is only valid at low frequencies. For a folded system, the amplification of the effect on the signal for gravitational waves decreases above a frequency  $\approx c/2LN$ , since there are fewer roundtrips per wave cycle. Thus the apparent gravitational wave spectrum actually rises from there up to a frequency  $\approx c/2L$ , above which it is about the same as an unfolded system. At  $f \approx c/2L$ , both types of system have an effective spectral amplitude  $h \approx \sqrt{t_P}$ , which just corresponds to  $\Delta L \approx \sqrt{Lt_P}$ . At frequencies above  $\approx c/2L$ , the apparent strain noise spectrum turns over to  $h(f) \propto (c/fL)\sqrt{t_P}$ . For example, holographic noise should appear in LIGO as an apparent (but illusory) stochastic gravitational-wave background at high frequency, with a maximum amplitude near the free spectral range of the system. Even though the system is dominated by photon shot noise at high frequencies, the holographic effect could be detected in principle using correlations between the two LIGO Hanford interferometers, using the technique discussed below.

### Cross Correlation of Two Instruments

An experiment designed to provide convincing evidence for or against the holographic hypothesis could include more than one interferometer. Two separate interferometers, with no physical connection aside from inhabiting the same holographic spacetime, should nevertheless show correlated holographic noise. This feature can be used to design an experiment with purely holographic signatures in the signal.

Consider two aligned interferometers, both with arms of length  $L$  parallel to the  $x$  and  $y$  axes. Suppose one is placed vertically above the other, with vertical displacement  $\Delta L_z$ . If  $\Delta L_z \ll L$ , the holographic position displacements of the two beamsplitters are almost the same.

To see that this coherence must occur, consider the holographic frame with wavefronts aligned normal to the  $z$  axis, that is, parallel to the  $xy$  plane containing the two arms. The positions of the two instruments at null separation (at times differing by  $\Delta L_z/c$  in the lab frame) are described by data on the same holographic wavefront. The uncorrelated  $x, y$  holographic displacement between the two at any time along each axis is then given by the transverse uncertainty in this frame, which is only  $\Delta x \approx \Delta y \approx \sqrt{ct_0 \Delta L_z}$ ; the rest of the apparent motion must be correlated. Therefore, for  $\Delta L_z \ll L$ , the cross correlation must be nearly perfect; the spacetime wavefunctions for the differences of  $x$  and  $y$  between the two systems are very narrow compared to the total wavefunction width corresponding to  $\sqrt{ct_0 L}$ . This follows as long as the two transverse degrees of freedom are independent in any holographic frame, so it is a robust prediction. If  $\Delta L_z$  is not small compared with  $L$ , the prediction from this description is not precisely determined by this argument.

In the Matrix theory description, the correlation is expected insofar as the optical elements of the two interferometers are described by different sets of D0 branes on the same light sheets. They all share the same holographic wavefunction for their collective transverse position, the trace of the matrix including all the branes.

The cross correlation gradually disappears as the interferometers are separated. For zero vertical displacement, cross correlation power is added linearly when aligned laser beam wavefronts are traveling in both arms of both interferometers at the same time. If the in-plane displacement exceeds the arm length in either direction, the correlation disappears. This must be true from causality: correlations only arise if causal diamonds defined by light paths in the two machines share overlapping spacetime volumes. Using these criteria, we can make a guess at the approximate cross correlation behavior for displacements along the arm directions. For two aligned interferometers offset along either arm by  $\Delta L$ , we guess at a cross correlation roughly of the form

$$\Xi_{\times}(\tau) = (ct_0/2\pi)(2L - 2\Delta L - c\tau), \quad 0 < c\tau < 2L - 2\Delta L \quad (36)$$

$$= 0, \quad c\tau > 2L - 2\Delta L. \quad (37)$$

These formulas likely describe the decorrelation accurately for small displacements, and possibly for large displacements along one axis, but the framework here does not suffice to treat the projection factors for general displacements in three dimensions. Projection effects will add geometrical factors of order unity.

The frequency spectrum of the cross correlation signal is given as above using the Wiener formula. For  $\Delta L > 0$ , the noise power is reduced at all frequencies. The low frequency limit becomes

$$\Phi_{\times}(f) \approx 4t_P L^2 [1 - (\Delta L/L)]/\pi, \quad f \ll c/2L. \quad (38)$$



## EXPERIMENTAL PROGRAM

It appears that an experiment that reaches this level of position sensitivity is guaranteed to provide informative results about physics at the Planck scale. That is, a null result excluding cross correlated noise in two systems, in contradiction to holographic theories, will imply in this interpretation that at least one of the two features outlined above (Planck frequency bound, or holographic information bound) does not hold. A positive result of course opens up a whole field of followup experiments that will illuminate the way that Planck-scale quantum physics maps onto the macroscopic, quasi-classical world.

A new experiment is therefore motivated to test the holographic hypothesis, using the predicted correlation between two close but not connected interferometers. For two aligned interferometers with a fractionally small displacement, a cross correlation in the holographic noise displacement is robustly predicted on general theoretical grounds. The two interferometers can be in separate cavities and Faraday isolated to exclude other sources of in-common noise in the relevant band. The dominant noise source, photon shot noise, is uncorrelated between the two and averages in time to zero, while the holographic noise is in common and averages to a definite known value. This allows an experiment on a much smaller scale (and higher frequencies) than the interferometric gravitational wave detectors, even though the photon shot noise dominates by a large factor at high frequencies.

Consider a pair of adjacent and aligned power-recycled interferometers. The time required for the cross correlation from holographic noise to equal the photon shot noise at frequency  $c/2L$  is [18]

$$t_{\gamma\times} \approx \left[ \frac{\lambda_{opt}^2}{L^3(2\pi)^4} \right] \left[ \frac{c^3}{\lambda_P^2} \right] \left[ \frac{h_P}{P_{opt}} \right]^2 \quad (39)$$

where  $\lambda_{opt}$  and  $P_{opt}$  refer to the wavelength and power of the laser cavity,  $h_P$  is Planck's constant, and  $L$  is the arm length. This becomes

$$t_{\gamma\times} \approx 375 \text{ s } (P_{opt}/1000\text{w})^{-2} (L/40\text{m})^{-3}. \quad (40)$$

Thus there is a trade between system size and laser power. The optimum appears to be a system with arms some tens of meters in length; for shorter arms, the large required power in the cavity and smaller waist size cause significant heating in the optics. For a system with 40m arms, the characteristic frequency is  $c/2L = 3.5$  MHz. With 1000 watt cavities, the correlated power matches the photon shot noise power after about  $t_{\gamma\times} \approx 5$  minutes. The significance of a detection after time  $t$  is about  $(t/t_{\gamma\times})^{1/2}$  standard deviations. Modern experimental techniques can sample and correlate data rapidly enough to study both time and frequency domain correlations in this regime.

For small fractional displacement between instruments, the predictions here are motivated on general grounds, but they become less reliable as the displacement approaches the apparatus size. If two close interferometers yield a positive result, a followup experimental program with different experimental geometries would inform this aspect of the theory.

I am grateful for discussions and correspondence with many colleagues, including particularly A. Chou, H. Grote, S. Hild, M. Jackson, C. Laemmerzahl, H. Lück, G. Mueller, Y. Ng, B. Schutz, J. Steffen, S. Tarabrin, S. Waldman, R. Weiss, S. Whitcomb, G. Woan, and other participants in the Hannover workshop on holographic noise, and for the hospitality of the Aspen Center for Physics. This work was supported by the Department of Energy.

- 
- [1] G. 't Hooft, "Dimensional reduction in quantum gravity," in "Conference on Particle and Condensed Matter Physics (Salamfest)", edited by A. Ali, J. Ellis, and S. Randjbar-Daemi (World Scientific, Singapore, 1993), arXiv:gr-qc/9310026.
  - [2] L. Susskind, "The World As A Hologram," J. Math. Phys. **36**, 6377 (1995)
  - [3] R. Bousso, "The holographic principle," Rev. Mod. Phys. **74**, 825 (2002)
  - [4] T. Banks, W. Fischler, S. H. Shenker and L. Susskind, "M theory as a matrix model: A conjecture," Phys. Rev. D **55**, 5112 (1997)
  - [5] C. J. Hogan, "Measurement of Quantum Fluctuations in Geometry" Phys. Rev. D **77**, 104031 (2008),
  - [6] C. J. Hogan, "Indeterminacy of Quantum Geometry" Phys Rev D.78.087501 (2008),
  - [7] J. R. Ellis, J. S. Hagelin, D. V. Nanopoulos and M. Srednicki, "Search For Violations Of Quantum Mechanics," Nucl. Phys. B **241**, 381 (1984).
  - [8] G. Amelino-Camelia, "Gravity-wave interferometers as probes of a low-energy effective quantum gravity," Phys. Rev. D **62**, 024015 (2000)
  - [9] G. Amelino-Camelia, "A phenomenological description of quantum-gravity-induced space-time noise," Nature **410**, 1065 (2001)

- [10] S. Schiller, C. Laemmerzahl, H. Mueller, C. Braxmaier, S. Herrmann and A. Peters, “Experimental limits for low-frequency space-time fluctuations from ultrastable optical resonators,” *Phys. Rev. D* **69**, 027504 (2004)
- [11] Y. J. Ng, “Quantum foam and quantum gravity phenomenology,” *Lect. Notes Phys.* **669**, 321 (2005)
- [12] L. Smolin, “Generic predictions of quantum theories of gravity,” arXiv:hep-th/0605052.
- [13] M. Srednicki, “Entropy and area,” *Phys. Rev. Lett.* **71**, 666 (1993)
- [14] C. J. Hogan and M. G. Jackson, “Holographic Geometry and Noise in Matrix Theory,” *Phys. Rev. D* **79**, 124009 (2009)
- [15] H. Kogelnik, T. Li, “Laser Beams and Resonators”, *Appl. Opt.* **5**, 1550 (1966)
- [16] A. E. Siegman, *Lasers*, Sausalito: University Science Books (1986).
- [17] J. B. Camp, N.J. Cornish, “Gravitational Wave Astronomy”, *Ann. Rev. Nuc. Part. Sci.* **54**, 525 (2004)
- [18] R. Weiss, “Concept for an interferometric test of Hogan’s quantum geometry hypothesis”, 2/10/2009.